Vegetation Forcing and Thermally Induced Generation of Mesoscale Circulation

X. Hong, M. J. Leach, and S. Raman
Department of Marine, Earth and Atmospheric Sciences
North Carolina State University
Raleigh, NC 27695-8208

Surface inhomogeneities, including boundaries between different types of vegetations and land use patterns, have important effects on the structure of the atmospheric boundary layer. Changes in the surface roughness, temperature and wetness make the planetary boundary layer (PBL) nonhomogeneous and produce substantial horizontal gradients of boundary layer properties. Significant differences in the surface thermal energy induce mesoscale circulations.

The presence of vegetation modulates the evaporation from the soil and enhances the vertical flux of water vapor into the PBL through transpiration. A realistic canopy formulation must ultimately represent the effects of vegetation on evaporation, energy partitioning, rainfall interception, and soil moisture, as well as albedo and aerodynamic roughness. Inclusion of canopy effects allows the deep-soil moisture (in the root zone) to act as a source for evapotranspiration.

Single-level canopy formulations are most appropriate for use in mesoscale models. We use a single-level canopy model (Deardorff 1978) that contains many parameters with which to evaluate fluxes from the soil beneath the canopy, from open areas between the canopy elements and from the foliage itself. This model can be used with a nonisothermal surface or a canopy for estimating vertical fluxes from the ground foliage system to the atmosphere.

This vegetation parameterization is included in a mesoscale model that has turbulent kinetic energy closure, explicit cloud physics, and a surface energy budget. The model is used to simulate mesoscale circulation between a vegetated area and a bare soil area. We also present the results of numerical experiments testing the sensitivity of mesoscale circulation to different underlying surface characteristics. For understanding the physical processes, the turbulent structure of the PBL is investigated as well.

Model Descriptions

We have incorporated a vegetation parameterization into the NCSU mesoscale numerical model using a modified version of Deardorff's (1978) soil-vegetation scheme. Several numerical experiments have been conducted using the NCSU model (Huang and Raman 1991,1992; Boybeyi and Raman 1992) to determine the validity of this model for different meteorological conditions and topographic features.

Deardorff's scheme provides for the heat and water exchanges at the land surface. It includes a representation of a vegetation layer that interacts both with the soil surface and the air temperature. Ground surface temperature and the moisture are obtained by solving simultaneously the energy budget and water budget equations at the soil vegetation-air interface, respectively. The scheme allows for two layers in the soil and a single vegetation canopy. The prognostic equations for the soil temperature and soil water content are described below.

The ground surface temperature T_g is calculated by a "force-restore" method:

$$\frac{\partial T_g}{\partial t} = -C_1 \frac{H_A}{\rho_s C_s d_1} C_2 \frac{T_g - T_2}{\tau_1} \quad (1)$$

The mean deep soil temperature T_2 is

$$\frac{\partial T_2}{\partial t} = - \frac{H_A}{\rho_s c_s d_2} \quad (2)$$

where H_A is the ground surface energy, ρ_s is the soil density and c_s is the soil thermal heat capacity.

The moisture budget equation that describes the vertical diffusion processes for the ground surface and the root layer is

$$\frac{\partial w_g}{\partial t} = -C_1 \frac{E_g + 0.1E_{tr} - P_g}{\rho_\omega d_1} - C_2 \frac{w_g - w_d}{\tau_1} \quad (3)$$

where w_g is volumetric concentration of soil moisture at the ground surface, and w_d is soil moisture content within the root layer. The time-dependent equation for w_d is

$$\frac{\partial w_d}{\partial t} = -\frac{E_g + E_{tr} - P_g}{\rho_\omega d_2} \quad (4)$$

where P_g is the precipitation rate at ground level.

The conservation equation for mass of liquid water retained by foliage is given by

$$\frac{\partial w_{dew}}{\partial t} = \sigma_f P - (E_f - E_{tr}) \quad 0 \le w_{dew} \le w_{d\,max} \quad (5)$$

where w_{dew} is mass of liquid water retained by foliage per unit horizontal ground area, w_{dmax} is maximum value of w_{dew} beyond which runoff to soil occurs.

Numerical Experiments and Results

Results of three numerical experiments designed to investigate the effect of different soil types in inducing mesoscale circulations between the vegetated area and the bare soil area are presented in this paper. The three soil types are clay, loam and sand. Different parameters used for the three soil types are shown in Table 1. The vegetation characteristics and initial atmospheric conditions are the same for all three experiments. The initial surface temperature is 300 K with a potential temperature lapse rate of +3.5 K/km. The ambient wind field is -1.0 m/s The starting time of the experiments is 0800 local time for mid-summer conditions.

Differential soil heat capacity creates differences in the sensible heat flux from the ground to the atmosphere. However, there is a larger latent heat flux from the vegetated area as the vegetation efficiently pumps moisture into the atmosphere from the root zone. All three cases exhibit the same general characteristics. The strength of the mesoscale circulation varies as the bare soil characteristics change. Sandy soil has the lowest heat capacity and the highest albedo of the three soil types.

The mesoscale circulation that develops due to the differences between a vegetated area and sandy soil is the strongest of the three cases and is shown in Figure 1. The upper frame is the u component of the wind superimposed on the potential temperature field. The u component shown has the initial -1.0 m/s wind subtracted to highlight the induced circulation. The lower frame is the v component of the wind with the actual temperature. The thermal fields show the creation of the baroclinicity in the boundary layer and also well-mixed layers to approximately 2 km. The effect of the stronger surface sensible heat flux is evident as the ground temperature is as much as 15°C greater over the sandy soil. The differential heating throughout the boundary layer drives the convergence zone at the interface between the bare soil and the vegetated area, with return flow at the top of the boundary layer.

The effects on moisture and vertical velocity are shown in Figure 2. The vertical velocity is superimposed on the specific humidity. The vertical velocities are consistent with the horizontal velocities with maximum values where the horizontal convergence is greatest. There is much more moisture through most of the boundary layer as vegetation effectively enhances the latent heat flux due to the transpiration from the root zone.

Table 1. Soil characteristics (K_s is the soil thermal diffusivity, ρ_s is the soil density, and c_s is the specific heat of the soil.).

Soil Type	Sand	Loam	Clay
Ks (m^2-s^{-1})	0.002×10^{-4}	0.0015×10^{-4}	0.012×10^{-4}
$\rho_s c_s$ ($Jm^{-3}K^{-1}$)	1.2558×10^6	4.186×10^6	2.3×10^6

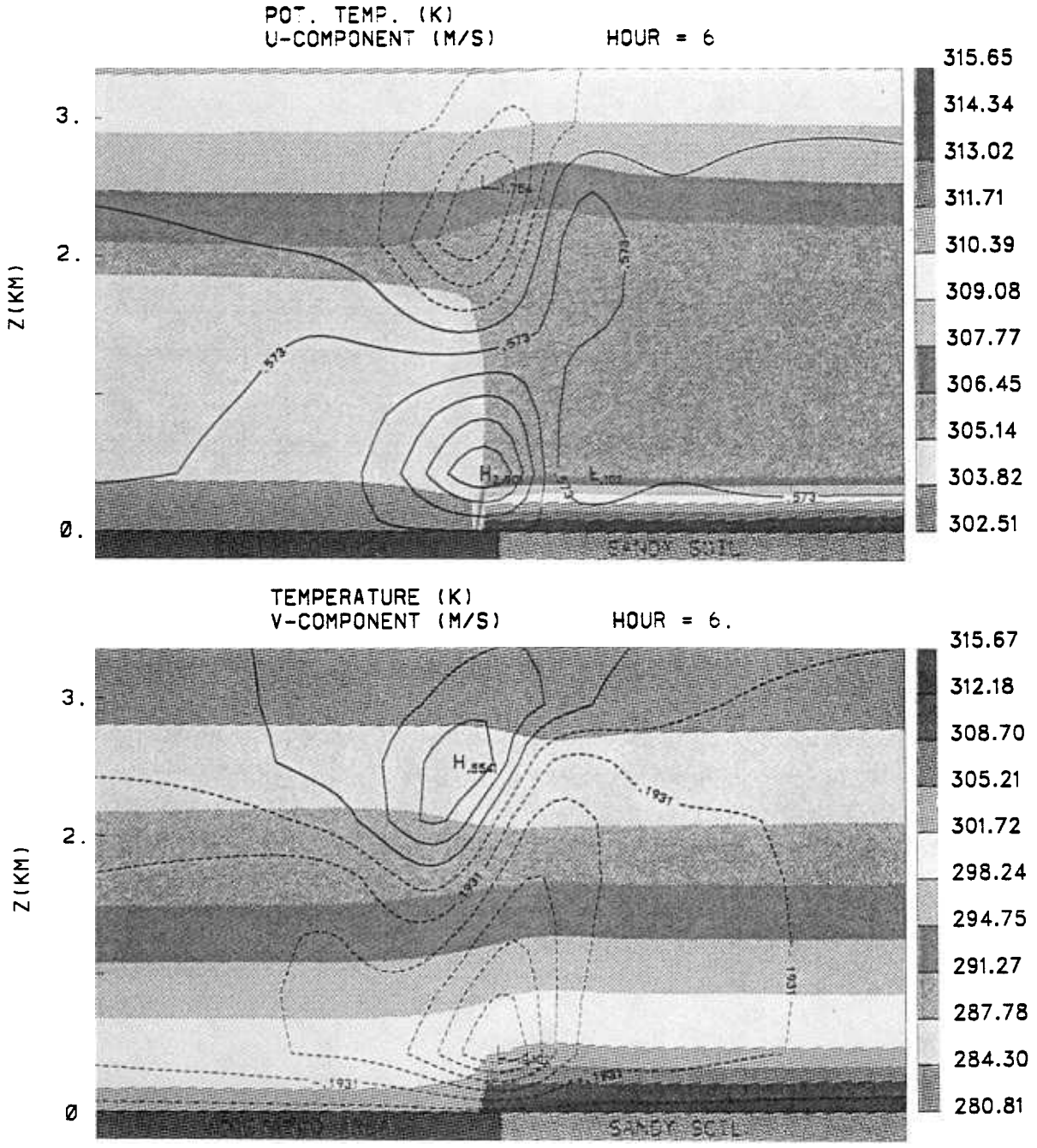

Figure 1. The upper panel is the u wind superimposed on the potential temperature, the lower panel is the v wind with the actual temperature. The results are from a 6-hour simulation with the mesoscale model. The vegetated area is on the left, sandy bare soil is on the right.

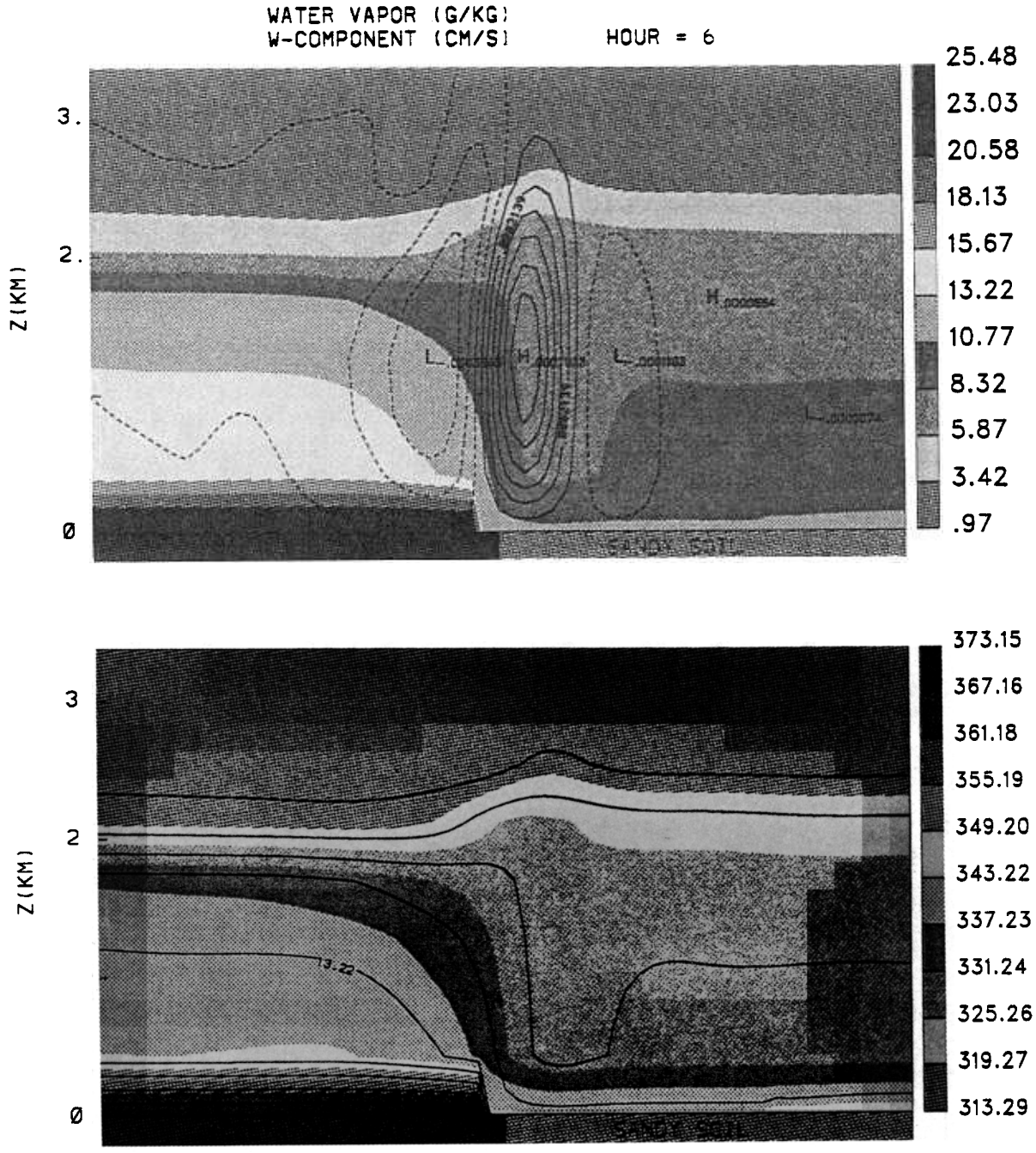

Figure 2. The upper panel is the w wind superimposed on the potential temperature, the lower panel is the v wind with the actual temperature. The results are from a 6-hour simulation with the mesoscale model. The vegetated area is on the left, sandy bare soil is on the right.

The effects on turbulence characteristics are shown Figure 3. The upper frame is the turbulent kinetic energy (TKE) and eddy diffusivity for momentum (K_M), the lower frame is the dissipation (ε) of TKE with the eddy diffusivity for heat (K_H) superimposed. The greater buoyancy production over the bare soil leads to much greater TKE, which in turn leads to greater mixing throughout the boundary layer. One could also infer this from the K_M and K_H distributions.

As mentioned, all three cases produced similar results. The differences among the cases were in the intensity of the circulation that developed, the timing of the onset of the circulation, and the subsequent development of a return circulation at the top of the PBL. The features of the three cases are presented in Table 2. The strongest circulation is associated with the sandy soil, which has the lowest heat capacity but the highest albedo of the three soil types. The weakest circulation is with the clay soil, which has the highest heat capacity.

Summary and Future Work

The results discussed above indicate the effects of different surface characteristics, such as vegetation and bare soil heat capacity, on thermally induced mesoscale circulation. Vegetation increases water vapor flux in the boundary layer but decreases the sensible heat flux. Soils with different heat capacities alter the transfer of heat fluxes to the atmosphere, affecting the PBL structure. Soils with smaller heat capacity transfer more sensible heat, producing more TKE, larger eddy diffusivity, and greater boundary layer heights. Our results indicate that the same vegetation cover with different bare soil combinations changes the strength and size of the mesoscale circulation.

In the future, we will extend the model to three dimensions, determine the effect of different soil covers and soil moisture on precipitation production, and couple the model with soil hydrology. We will use land use patterns from North Carolina and Oklahoma. These regions are two of the locales chosen for the U.S. Department of Energy's Atmospheric Radiation Measurement (ARM) Program. Observations from the 1991 and 1992 Boardman Regional Flux Experiment will also be used to validate the model. Effects of the resulting mesoscale circulation on the water budget, hydrology, and radiation budget will then be investigated.

Acknowledgments

This work is supported by the U.S. Department of Energy's ARM Program, under contract number 091575-A-QI with Pacific Northwest Laboratory. Computer time was provided by the DOE at the National Energy Research Supercomputer Center and by the North Carolina Supercomputing Center.

References

Boybeyi, Z., and S. Raman. 1992. A three-dimensional numerical sensitivity study of convection over the Florida peninsula. *Bound.-Layer Meteorol.* **60**:325-359.

Deardorff, J. W. 1978. Efficient prediction of ground surface temperature and moisture, with inclusion of a layer of vegetation. *J. Geophys. Res.* **20**:1889-1903.

Garratt, J. R. 1992. *The atmospheric boundary layer.* Cambridge University Press.

Huang, C.-Y., and S. Raman. 1991. Numerical simulation of January 28 cold air outbreak during GALE, Part I: The model and sensitivity tests of turbulence closures. *Bound.-Layer Meterol.* **55**:381-407, 1991.

Huang, C.-Y., and S. Raman. 1992. A three-dimensional numerical investigation of a Carolina coastal front and the Gulf Stream rainband. *J. Atmos. Sci.* **49**(7):560-584.

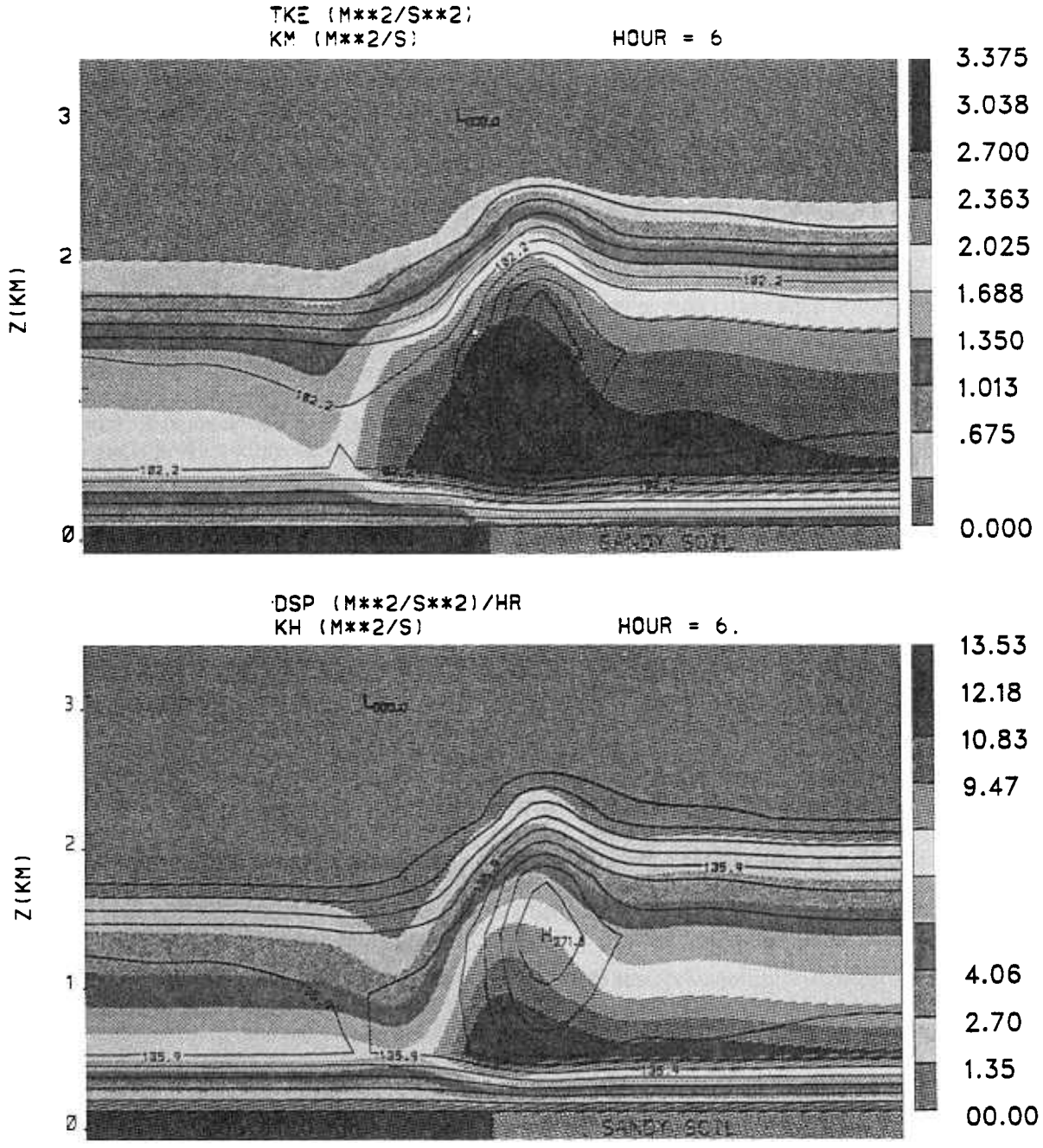

Figure 3. The upper panel is the momentum eddy diffusivity superimposed on the turbulent kinetic energy (TKE), the lower panel is the scale eddy diffusivity with the dissipation of TKE. The results are from a 6-hour simulation with the mesoscale model. The vegetated area is on the left, sandy bare soil is on the right.

Table 2. Characteristics of the circulation and PBL in experiments with three soil types.

Characteristic	Sand	Loam	Clay
U_{max} (m/s)	2.9	1.8	0.8 (not closed)
U_{min} (return)	-1.7	-0.9	-0.4
V_{max} (return)	0.6	0.2	0.1
V_{min}	-0.9	-0.3	-0.3
TKE (m**2/s**2)	3.4	2.7	1.7
K_M (m**2/s)	204.4	132.3	82.5
K_H	271.8	173.6	110.5
T_{onset} (hour)	1	2	5
T_{return}	2	3	6

(a) All results are for 6-hour simulation time, except the last two rows which are the estimated time of onset of the mesoscale circulation and the development of the return flow at the top of the PBL, respectively.